Synthesis, crystal structure, Hirshfeld surface, computational and antibacterial studies of a 9-phenanthrenecarboxaldehyde-based thiodihydropyrimidine derivative

A.E. Huseynzada[1,2,3*], M. Mori[4], F. Meneghetti[4], A. Israyilova[2,5,11], G. Tuzun[6], K. Sayin[6], L. R. Chiarelli[7], C. Mutlu[8], M. Demiralp[9], U.A. Hasanova[1,2], V. Abbasov[10]

[1]ICRL, Baku State University, Z. Khalilov 23, Baku, AZ 1148, Azerbaijan

[2]GPOGC SRI, Azerbaijan State Oil and Industry University, Baku, Azerbaijan

[3]Chemistry Department, Azerbaijan Engineers Union, Bashir Safaroglu 118, Baku, Azerbaijan

[4]Department of Pharmaceutical Sciences, University of Milan, Via L. Mangiagalli 25, 20133 Milano, Italy

[5]Laboratory of Microbiology and Virology, Baku State University, Z. Khalilov 23, Baku, AZ 1148, Azerbaijan

[6]Chemistry Department, Sivas Cumhuriyet University, Sivas, Turkey

[7]Department of Biology and Biotechnology, University of Pavia, Via Ferrata 9, 27100 Pavia, Italy

[8]Department of Chemistry, Gebze Technical University, Kocaeli, Turkey

[9]Advanced Technology Research and Application Center, Sivas Cumhuriyet University, Sivas, Turkey

[10]Institute of Petrochemical Processes, K. Avenue 30, Baku, AZ 1005, Azerbaijan

[11]Research Institute of Crop Husbandry, Ministry of Agriculture, Baku, Azerbaijan.

[*]corresponding author e-mail: alakbar.huseynzada1117@gmail.com

Abstract

We report herein the synthesis of a new biologically active 3,4-dihydropyrimidin-2(1*H*)-thione derivative (**4**) from 9-phenanthrenecarboxaldehyde, thiourea, and methyl acetoacetate by the Biginelli reaction. The structure of the synthesized compound was investigated by NMR spectroscopy, mass spectrometry, and elemental analysis. Moreover, to gain insight into the conformation and crystal packing, the structure of the novel dihydropyrimidine was also studied by single-crystal X-ray diffraction. The Hirshfeld surface and contact enrichment analyses were used to better understand the molecular interactions. Considering the biological activity of dihydropyrimidines, the antibacterial effect of the synthesized compound was evaluated against *A. baumanii, E. coli, P.aeruginosa, K. pneumoniae*, and *S. aureus*; interestingly, high activity was detected against *S. aureus*. Additionally, computational studies were performed using the Gaussian package and the Maestro Schrodinger programs, and the theoretical IR and NMR spectra of compound **4** were examined. Finally, an ADME/T analysis was performed to estimate the drug-likeness of the compound.

Keywords: thiodihydropyrimidine, Hirshfeld surface analysis, crystal structure, molecular docking, ADME/T.

1. Introduction

One-pot multicomponent reactions represent a potent synthetic method and a versatile, multifaceted tool for the production of a wide range of molecules with a broad spectrum of activities. Multicomponent reactions are gaining popularity day by day because they provide synthetic chemists with a number of extraordinary "trump cards" over traditional linear synthesis, including ease of use, simplicity of starting building blocks, high level of product complexity, and broad diversification [1-3]. The three-component, one-pot Biginelli reaction, which was discovered by the Italian chemist Pietro Biginelli in 1893, belongs to this type of transformation. This approach has found application in the synthesis of dihydropyrimidines, a class of two-nitrogen-containing six-membered heterocycles. This reaction, which is a combination of an aldehyde, a methylene-active compound, and a urea derivative, has been intensively studied, becoming increasingly popular among medicinal chemists after the discovery of the biological activities of dihydropyrimidines, which constitute ideal drug candidates. Another "ace up the sleeve" of the Biginelli reaction is the ease of introduction of various pharmacophoric groups in the structure of dihydropyrimidines, allowing their easy modification and the creation of hybrid molecules to enhance the range of their biological activities [4-9]. As a result, various investigations performed by scientists from all over the world have led to the obtainment of antitubercular compounds [10], mPGES-1 inhibitors [11], antidiabetic, antimalarial [12], antiepileptic [13], anti-HIV [14], anti-hypertensive [15-19], anti-inflammatory [20-22], antibacterial [23-26], antitumor [27-32], anti-leishmanial, antiproliferative [33], antiviral, antifungal [8, 9] agents, miscellaneous [34-36], potassium [37-39] and calcium channel and α_{1a}adrenergic antagonists [40]. However, this broad spectrum of biological activities is not the only reason why this class of compounds is a promising source of drug candidates. A "business card" of dihydropyrimidines that confirms their suitability as drugs is their presence in the structures of several therapeutic agents, including (*S*)-monastrol [41], 5-fluorouracil [42, 43], (S)-enastron [31], mon-97 [44], (*R*)-fluorastrol for the treatment of cancer [45], batzelladine A and B for the treatment of HIV [14], terazosin for the treatment of benign prostatic hyperplasia and high blood pressure [43], riboflavin (dietary supplement) [46], idoxuridine for the treatment of herpesvirus [47, 48], aminophylline for the treatment of asthma or COPD-based airway obstruction [49], methylthiouracil as antithyroid preparation [50]. Overall, these advantages have encouraged scientists to optimize synthetic methods to produce dihydropyrimidines, searching for innovative catalysts and constructing new molecules from different building blocks by employing the Biginelli reaction. To gain a deeper insight into the stereochemistry, conformation, and non-covalent interactions between molecules, which are key factors affecting activity, various methods have been used, leading to the development, enhancement and enrichment of their chemistry [51-53]. Furthermore, theoretical calculations have been frequently used to predict and/or explain their activities by finding the relationship between the structure of the investigated molecule and its biological effect [54, 55].

In this work, a new thiourea-based dihydropyrimidine derivative was synthesized from 9-phenanthrenecarboxaldehyde by a microwave-mediated Biginelli reaction in the presence of cerium chloride. Because crystals of this compound were obtained, its structure was investigated by single-crystal X-ray diffraction (SC-XRD). In addition, the Hirshfeld surface and contact enrichment analyses were performed to quantify the molecular interactions and understand their importance in the crystal packing. Moreover, due to the fact that dihydropyrimidines demonstrate a wide spectrum of biological activities, the antibacterial effect of the compound was analyzed against Gram-positive (*S. aureus*) and Gram-negative bacteria (*A. baumanii*, *E. coli*, *P.aeruginosa*, *K. pneumoniae*), leading to promising results. Finally, computational studies of the novel dihydropyrimidine derivative were performed on the b3lyp/6-31g(d) basis set. Calculated IR and NMR spectra of the molecule were compared to the experimental data and examined in detail. Subsequently, molecular docking calculations were carried out using *Staphylococcus aureus* (PDB ID: 3G7B) [56], *Pseudomonas aeruginosa* (PDB ID: 2UV0) [57], and *Escherichia coli* proteins (PDB ID: 4WUB) [58].

2. Materials and methods

2.1 General Information

All solvents and reagents, purchased from commercial suppliers, were of analytical grade and used without further purification. The control of the reaction progress and the determination of the purity of the synthesized compounds was done by thin-layer chromatography (TLC) on Merck silica gel plates (60 F254 aluminium sheets), visualized under UV light. Melting points were recorded in open capillary tubes on a Buchi B-540 apparatus and were uncorrected. Elemental analysis was performed on a Carlo Erba 1108 analyzer.

2.2 Experimental synthesis procedure

*Synthesis of 6-methyl-4-(phenanthren-9-yl)-2-thioxo-1,2,3,4-tetrahydropyrimidine-5-carboxylate (**4**) by the Biginelli reaction (Scheme 1).*

0.5 mmol (103 mg) of 9-phenanthrenecarboxaldehyde (**1**), 0.79 mmol (60 mg) of thiourea (**2**), and 0.147 mmol (0.055 mg) of $CeCl_3 \cdot 7H_2O$ were added to a microwave vial with a magnetic stirrer and dissolved in 1 mL of ethanol. Subsequently, 0.556 mmol (60 µl) of methyl acetoacetate (**3**) was added to a vial, which was sealed and irradiated at 100 ° C in a microwave reactor for 2.5 h at a maximum power of 200 W (CEM Discover System). At the end of the reaction time, the yellow precipitate (in the absence of a precipitate, the solvent was partially evaporated to facilitate the formation of the solid) was filtered, washed with distilled water, and dried. The purity of the compound was 90%, at this step. Further purification of **4** was performed by the Biotage Isolera One Flash Chromatography System (cyclohexane-ethyl acetate-methanol) using both the reaction solution and the precipitate. After purification and removal of the solvent, a yellow solid was obtained. Single crystals of **4** were grown by crystallization from a methanol-ethyl acetate mixture (4:1). Yield: 68 %. M.p.: 254.1 °C. **^{1}H NMR** (DMSO-d_6, δ, ppm): 2.53 (s,

3H, CH_3), 3.42 (s, 3H, OCH_3), 6.14-6.15 (s, 1H, CH), 7.60-7.78 (m, 5H, $5C_{Ar}H$,), 7.97-8.00 (d, *J* = 9 Hz, 1H, $1C_{Ar}H$), 8.51-8.54 (t, *J* = 6 Hz, 1H, $C_{Ar}H$), 8.80-8.92 (m, 2H, $2C_{Ar}H$), 9.72 (s, 1H, NH), 10.50 (s, 1H, NH). **^{13}C NMR** (DMSO-d_6, δ, ppm): 17.37 (CH_3), 50.1 (CH), 51.07 (OCH_3), 99.63 (C), 122.73 ($C_{Ar}H$), 123.46 ($C_{Ar}H$), 124.47 ($C_{Ar}H$), 125.21 ($C_{Ar}H$), 125.53 ($C_{Ar}H$), 126.82 ($C_{Ar}H$), 126.99 ($C_{Ar}H$), 127.32 ($C_{Ar}H$), 128.89 ($C_{Ar}H$), 129.04 (C), 129.75 (C_{Ar}), 130.46 (C_{Ar}), 130.78 (C_{Ar}), 136.09 (C_{Ar}), 146.55 (C_{Ar}), 165.57 (COO), 174.04 (CS). HRMS (ESI- MS): 363.17 $[M+H]^+$ (Figure S1-S4). Elemental analysis calcd. for $C_{21}H_{18}N_2O_2S$, %: C, 69.59; H, 5.01; N, 7.73. Found, %: C, 69.69; H, 5.13; N, 7.81.

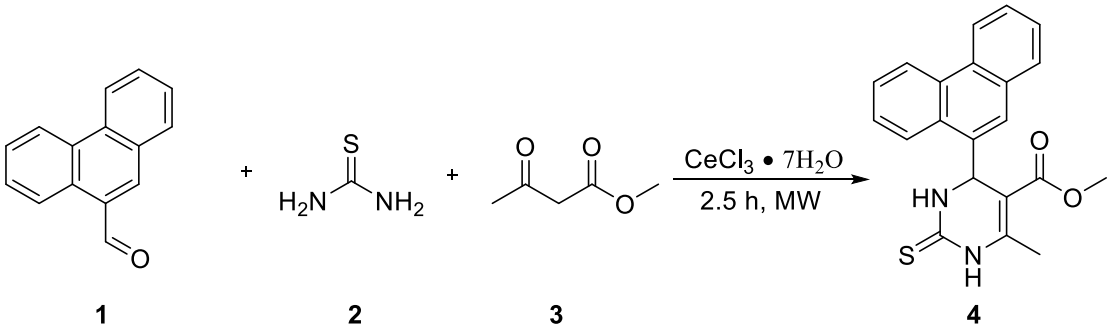

1 **2** **3** **4**

Scheme 1. Synthesis of the title dihydropyrimidine (**4**).

2.3 NMR experiments

The NMR experiments were performed on a BRUKER FT NMR spectrometer AVANCE 300 (Bruker, Karlsruhe, Germany) (300 MHz for ^{1}H and 75 MHz for ^{13}C) with a BVT 3200 variable temperature unit in 5 mm sample tubes using Bruker Standard software (TopSpin 3.1). Chemical shifts are given in ppm (δ) and are referenced to internal tetramethylsilane (TMS). Multiplicities are declared as follows: s (singlet), d (doublet), t (triplet), and m (multiplet). Coupling constants *J* are given in Hz. The experimental parameters for ^{1}H are as follows: digital resolution = 0.23 Hz, SWH = 7530 Hz, TD = 32 K, SI = 16 K, 90° pulse-length = 10 ms, *PL*1 = 3 dB, *ns* = 1, *ds* = 0, *d*1 = 1 s and for ^{13}C as follows: digital resolution = 0.27 Hz, SWH = 17985 Hz, *TD* = 64 K, *SI* = 32 K, 90° pulse-length = 9 ms, *PL*1 = 1.5 dB, *ns* = 300, *ds* = 2, *d1* = 3 s. NMR-grade DMSO-d_6 (99.7%, containing 0.3% H_2O) was used to solubilize the synthesized compound.

2.4 Mass experiments

High-resolution mass spectrometry (HRMS) was performed using electrospray ionization (ESI) in positive-ion detection mode.

2.5 X-Ray analysis

X-Ray analyses were performed on a Bruker SMART APEX II Single Crystal X-ray Diffractometer equipped with graphite-monochromated Mo-Kα radiation (λ = 0.71073 Å). The crystal structure was solved by direct methods and refined on F^2 by full-matrix least-squares using Bruker's SHELXTL-97 [59]. The details of the crystallographic data for the synthesized compound are summarized in Table 1. Crystallographic data for the structural analysis were

deposited to the Cambridge Crystallographic Data Center under accession number CCDC 2103266. The refined structure was inspected using ORTEP-3 (v. 2020.1) [60] and analyzed by Mercury 4.0 (v. 2021.3.0) [61] and PARST [62], within the WinGX suite (v. 2021.3) [60]. Graphical representations were rendered with Mercury.

2.6. Hirshfeld surface analysis

Hirshfeld surfaces and two-dimensional fingerprint plots were generated using CrystalExplorer21 (v. 21.5) [63]. Contact enrichment analysis was performed using MoProViewer (v. 1.2000) [64]; details are provided in the Supplementary Materials.

2.7. Antibacterial activity

The disc diffusion method, as reported by Mayrhofer [68], was used to screen the antibacterial activity of compound **4**. In detail, 1 mL of the fresh bacterial suspension was swabbed (10^5 CFU/mL) on the surface of the nutrient medium (Mueller Hinton Agar (MHA)), and plates were used 15 min after preparation. The test compound was solubilized in DMSO, and discs with certain concentrations were stratified on the surface of the nutrient medium using sterile tweezers. Plates were incubated at 37 °C for 24 h. The inhibition zones were measured and compared to those of control plates without the compound and with the known drugs cefotaxime and ceftriaxone.

The minimum inhibitory concentration of the test compound was determined by the two-fold microdilution method [65-67], using resazurin dye, in accordance with CLSI guidelines [87]. The compounds were prepared according to CLSI standards and diluted in U-bottom 96-well microtiter plates containing Muller Hinton Broth (MHB). The bacterial strains were prepared freshly from overnight cultures. The final density of test cultures was adjusted to 10^5 CFU (colony forming units) by using a digital densitometer. The bacterial suspension was added to each well of the microplate and incubated at 37 °C for 24 h. As a result, the concentration of the tested compound ranged from 1000 to 7.8 μg/mL. The growth of the bacterial cells was determined by the resazurin method. After incubation, 30 μL of resazurin dye (0.01 %) (Sigma Aldrich) was added to each well, and the microplates were again placed in an incubator for 3-4 h. The minimum inhibitory concentration (MIC) was defined as the lowest concentration of compound that prevented a color-change from blue to pink (bacterial growth was indicated by the pink color). The MIC value of the studied compound was compared with that of ceftriaxone.

2.8 Computational Approach

The calculation on the Gaussian software program was made in B3LYP with the 6-31g(d) basis set [69, 70]. Quantum chemical parameters, including HOMO (Highest Occupied Molecular Orbital), LUMO (Lowest Unoccupied Molecular Orbital), ΔE (HOMO-LUMO energy gap), chemical potential (μ), electrophilicity (ω), chemical hardness (η), global softness (σ), nucleophilicity (ε), dipole moment, and energy values were calculated using the below-given equations [71]:

$$\chi = -\left(\frac{\partial \mathrm{E}}{\partial \mathrm{N}}\right)_{v(r)} = \frac{1}{2}(I + A) \cong -\frac{1}{2}(E_{HOMO} + E_{LUMO})$$

$$\eta = -\left(\frac{\partial^2 \mathrm{E}}{\partial \mathrm{N}^2}\right)_{v(r)} = \frac{1}{2}(I - A) \cong -\frac{1}{2}(E_{HOMO} - E_{LUMO})$$

$$\sigma = 1/\eta \qquad \omega = \chi^2/2\eta \qquad \varepsilon = 1/\omega$$

The program developed by the Maestro Molecular modelling platform (version 12.8) by Schrödinger [72] was used for molecular docking simulations. Calculations were made up of several steps, each performed differently. In the first step, the "protein preparation module" [73] was used for the determination of the active sites of the proteins. The next step was the preparation of the compound. For this purpose, the molecule was first optimized with the Gaussian software, and then the LigPrep module [74] was employed for the calculations using the optimized structure. The Glide ligand docking module [75] was used to examine the interactions between the molecule and the target proteins from *Staphylococcus aureus* (PDB ID: 3G7B) [56], *Pseudomonas aeruginosa* (PDB ID: 2UV0) [57], and *Escherichia coli* (PDB ID: 4WUB) [58]. Calculations were performed using the OPLS4 method. Finally, an ADME/T analysis (absorption, distribution, metabolism, excretion, and toxicity) was performed to examine the druglikeness of the compound. The Qik-prop module [76] of the Schrödinger software was used to predict the effects and transformations of the molecule after human metabolism.

3. Results and discussion

3.1 Chemical synthesis.

A large number of procedures have been developed for the Biginelli reaction, resulting in the synthesis of dihydropyrimidines in high yields and with simple work-up techniques. In the present case, several catalysts including $Cu(OTf)_2$, $InCl_3$, $InBr_3$, CF_3COOH, $Yb(OTf)_3$, $YbCl_3$, HCl, H_2SO_4, NH_4Cl, CAN, CH_3COOH, $CH_2ClCOOH$ and others did not lead to the desired compound [8]. We were only able to obtain the title dihydropyrimidine by improving a literature procedure [52] and performing the reaction under microwave irradiation (Scheme 1). The structure of the newly synthesized dihydropyrimidine was determined by ^1H, ^{13}C NMR, mass spectrometry, and elemental analysis. As it can be seen from the ^1H NMR spectrum, the signals from the methyl and methoxy groups are observed at 2.53 and 3.42 ppm, respectively, whereas the CH group is at 6.14 ppm. Their positions in the ^{13}C NMR spectrum are at 17.37, 50.1, and 51.07 ppm. The signals from amine groups of the dihydropyrimidine core are observed at 9.72 and 10.5 ppm, whereas the positions of the ester and thiocarbonyl group are at 165.57 and 174.04 ppm, respectively (Figure 1S-4S).

3.2 Structure description.

Single crystals of the title compound were obtained by the slow evaporation of a methanol-ethyl acetate (8:1) solution, after 4 weeks. Crystallographic data and refinement details are given in Table 1.

Table 1. Crystal data and structural parameters of compound **4**.

Crystal data	
Chemical formula	$C_{21}H_{18}N_2O_2S$
M_r	362.43
Crystal system, space group	Monoclinic, P 1 2_1/n 1
Temperature (K)	120.03
a, *b*, *c* (Å)	5.0021(19), 29.981(11), 23.097(8)
B (°)	93.209(9)
V (Å^3)	3458(2)
Z	8
Radiation type	Mo-Kα (λ = 0.71073 Å)
μ (mm^{-1})	0.206
Crystal size (mm)	0.28x0.05x0.03
Data collection	
Diffractometer	Bruker-Axs Smart-Apex CCD
Absorption correction	multi-scan
T_{min}, T_{max}	0.5189, 0.7452
No. of measured, independent and observed [$I > 2\sigma(I)$] reflections	25243, 6043, 1516
R_{int}	0.3725
Structure Refinement	
R, wR^2, S	0.0817 [$I > 2\sigma(I)$] and 0.3217 [all], 0.1373 [$I > 2\sigma(I)$] and 0.1751 [all], 0.715 [all]
No. of parameters	473
No. of restraints	534
$\Delta\rho_{max}$, $\Delta\rho_{min}$ (e Å^{-3})	0.491, -0.321

Compound **4** crystallized in the monoclinic space group $P2_1/n$ with two independent molecules (**I** and **II**) in the asymmetric unit, representing the two enantiomers of a racemic mixture. The structure is shown in Figure 1 as an ORTEP diagram, with the arbitrary atom-numbering scheme.

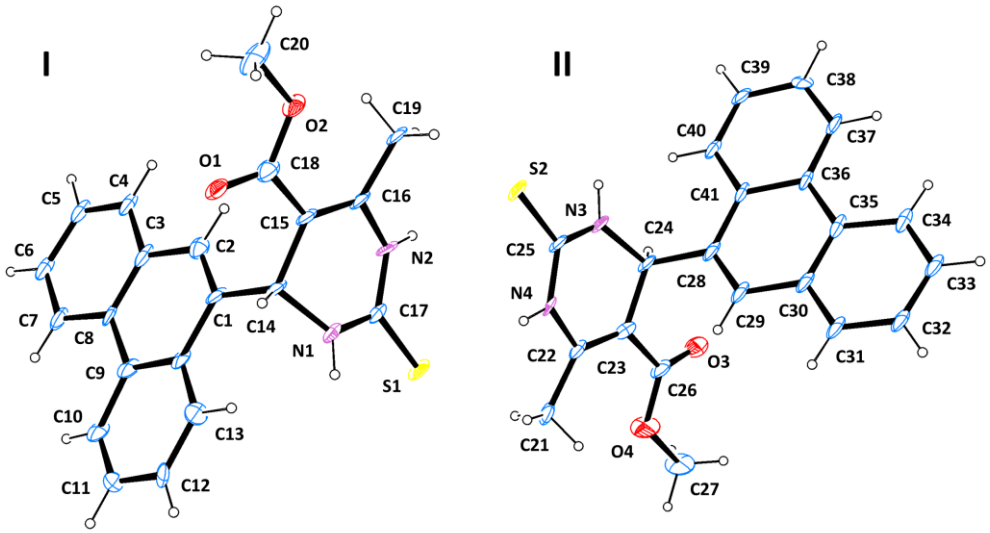

Figure 1. ORTEP diagram of **4** (**I** and **II**), with the arbitrary atom-numbering scheme. Thermal ellipsoids are drawn at the 40% probability level.

The molecular structure of **4** is characterized by a thiodihydropyrimidine nucleus bound to a phenanthrene moiety through an asymmetric carbon. Consequently, the angle between the best mean plane calculated for the heterocyclic ring and the aromatic portion is 80.6(5)° and 71.5(5)° for molecules **I** and **II**, respectively. In **I**, the maximum deviation from the weighted least-squares plane was observed for C14, with a distance of 0.189(4) Å; conversely, the most deviating atom in **II** is N3, with 0.121(1) Å. The plane formed by the methyl and methyl carboxylate substituents is inclined to the best mean plane of the dihydropyrimidine nucleus at an angle of 11.7(5)° and 6.7(8)° in **I** and **II**, respectively. Finally, the Cremer-Pople puckering parameters of the heterocyclic ring are $\theta = 108.41(5)°$, $\varphi = 160.29(5)°$, $Q_T = 0.3137(3)$ for **I**, and $\theta = 76.99(9)°$, $\varphi = -27.85(11)°$, $Q_T = 0.2058(4)$ for **II**, indicating a flattened boat conformation.

The two molecules in the asymmetric unit interact with each other through two long-range H-bonds between the sulfur atom of the thione and an NH group of the dihydropyrimidine ring. Non-traditional H-bonds are also established between the carbonyl oxygen of the ester and CH groups of the phenanthrene rings of adjacent molecules. All details are reported in Table 2. The crystal packing is consolidated by strong parallel π-π stacking interactions between the flat phenanthrene moieties: the planes on which the two aromatic portions lie are at 3.383(1) Å, and the distance between the centroids calculated for the phenanthrene rings is 5.002(1) Å. Minor CH···π and van der Waals contacts contribute to the stabilization of the crystal structure. Figure 2 provides a graphical depiction of the molecular packing.

Table 2. Hydrogen bonding geometry in the crystal structure of **4**.

H-bond	D-H/Å	H···A/Å	D···A/Å	D-H···A/°
N2-H2 S2	0.880	2.546(1)	3.342(1)	150.80(4)
N4-H4A S1	0.880	2.599(1)	3.433(1)	158.38(4)
C2-H2A O1	0.950	2.382(1)	3.246(1)	151.03(4)
C32-H32 O1	0.950	2.622(1)	3.551(1)	166.06(4)
C29-H29 O3	0.950	2.528(1)	3.446(1)	162.55(4)

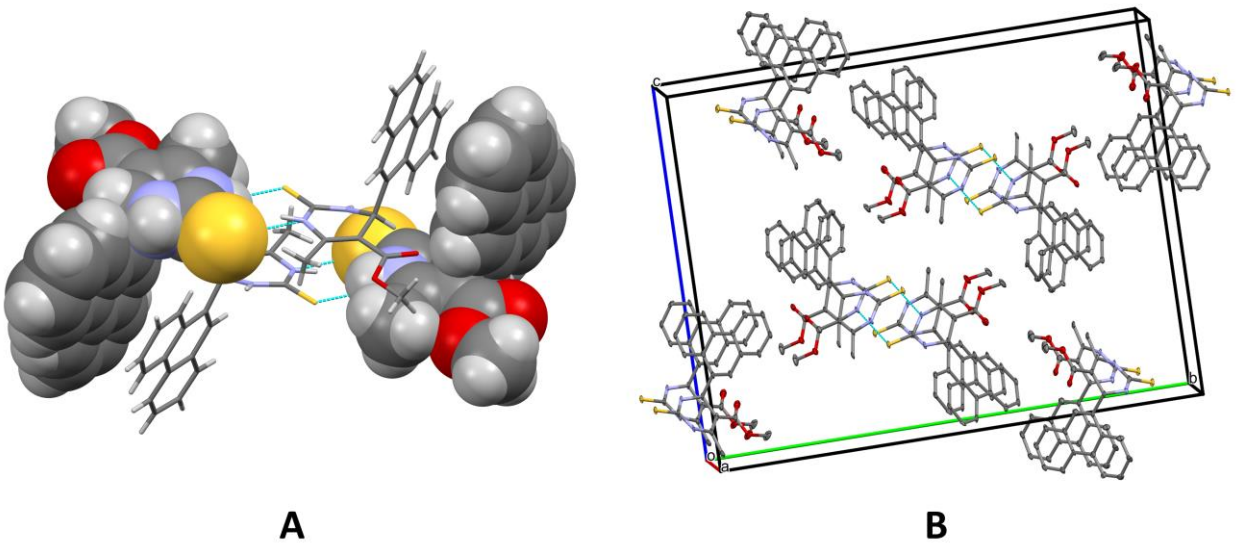

Figure 2. A. Spacefill-stick model of **4**, evidencing the main H-bonds and the π-π stacking interactions. **B.** Ellipsoid model (40% probability level) showing the crystal packing along the *a* axis. Hydrogen atoms are omitted for the sake of clarity.

3.3 Hirshfeld surface analysis

The Hirshfeld surface of the title dihydropyrimidine **4** was mapped over the normalized contact distance (d_{norm}), according to the following equation:

$$d_{norm} = \frac{d_i - r_i^{vdW}}{r_i^{vdW}} + \frac{d_e - r_e^{vdW}}{r_e^{vdW}}$$

where d_i is the distance between the HS and the nearest nucleus inside the surface, d_e is the distance between the HS and the nearest nucleus outside the surface, and r^{vdW} represents the van der Waals radius of the atom [77, 78]. The HS was calculated for the two independent molecules (**I** and **II**) in the asymmetric unit (Table 3): while their surfaces are not identical, they share most of the key characteristics. Hence, HS-**II** was arbitrarily chosen for the discussion, but the same concepts can be applied to HS-**I**, too.

Table 3. Characteristics of the two HS generated for the two independent molecules (**I** and **II**) in the asymmetric unit.

	V (Å³)	**A (Å²)**	***G***	***Ω***
HS-I	420.33	387.25	0.701	0.062
HS-II	428.17	383.48	0.716	0.059

The d_{norm} property was visualized with a red-blue-white color scheme, based on the length of the intermolecular contact with respect to the sum of the van der Waals radii. As shown in Figure 3A, the surface presents two big red spots corresponding to the H-bond established between the sulfur atom and one of the NH groups of the dihydropyrimidine nucleus. The remaining, generally feeble, red spots correspond to weak CH···O bonds, CH···π interactions, and other less significant short-range contacts. The HS of the compound mapped over the shape-index helped identify complementary portions in the crystal packing structure. As shown in Figure 3B, hollow regions perfectly match bumpy areas in the interacting molecules;

specifically, red spots indicate deep concavities corresponding to shorter-range contacts. Moreover, the characteristic pattern of red-blue triangles on the phenanthrene portion of the compound indicated the presence of strong parallel π-π stacking interactions. The large flat area evidenced by the curvedness plot (Figure 3C) confirmed the potential to form intermolecular aromatic–aromatic contacts.

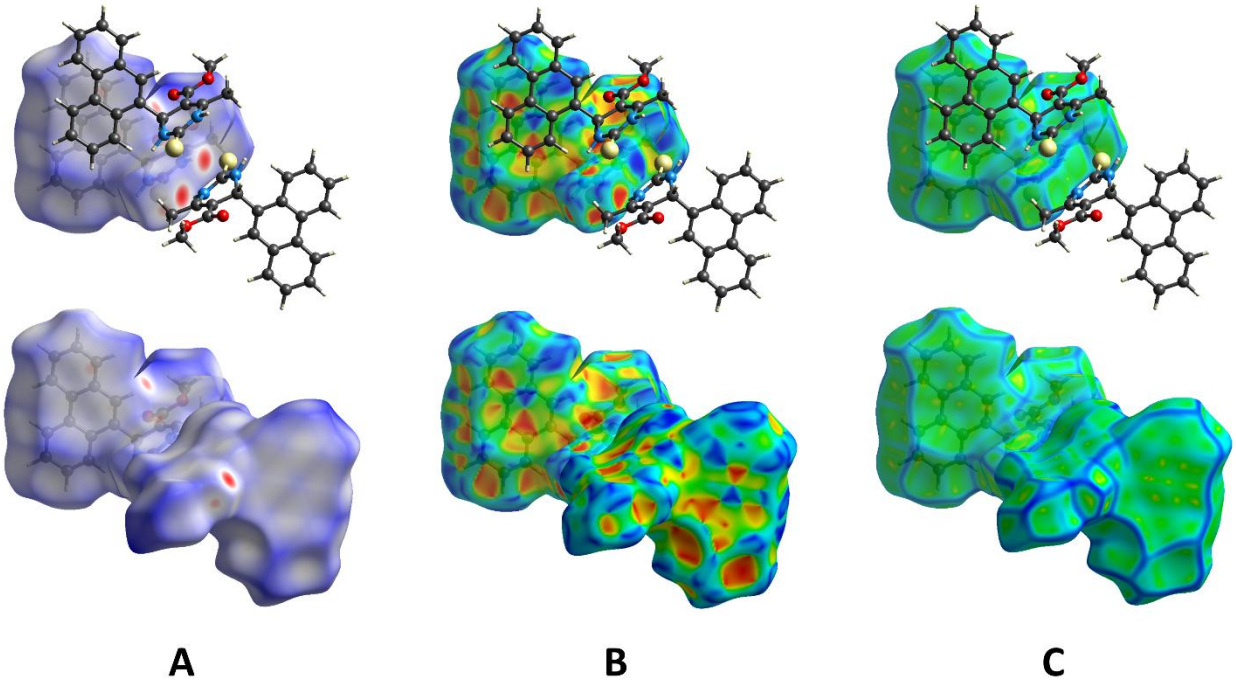

Figure 3. A. HS-**II** mapped over d_{norm} with a fixed colour scale in the range -0.3214 au (red) – 1.6319 au (blue), based on the length of the intermolecular contacts with respect to the sum of the van der Waals radii (red: shorter; blue: longer; white: same). **B.** HS-**II** mapped over the shape-index (colour scale: -0.9988 au – 0.9982 au). Blue areas represent bumps and red regions indicate hollows. **C.** HS-**II** mapped over the curvedness (colour scale: -3.7422 au – 0.4341 au). Green represents flat regions and blue indicates edges.

The two-dimensional (2D) fingerprint of HS-**II**, providing a visual summary of the contribution of each contact type and the relative area of the surface corresponding to it, revealed that H···H contacts are the major contributors, accounting for nearly half of the HS (46.6%). A considerable portion is also constituted by C···H/H···C contacts (19.8%), representing both van der Waals and CH···π interactions. The major determinants of the crystal packing are NH···S H-bonds and π-π stacking interactions. The former is evidenced by the S···H/H···S plot, accounting for 12.6% of the whole surface; the shape of the fingerprint is characterized by two spikes protruding towards the lower left part of the graph. Differently from those of traditional H-bonds, these spikes are short, reflecting the longer range of S···H contacts compared to O···H bonds. Stacking interactions can be easily inferred from the C···C plot (7.0%), which shows the characteristic arrow-shaped pattern with a central green region, indicating a rather large contribution of the points on the surface. Non-traditional H-bonds between the carbonyl oxygen of the ester and aromatic hydrogens represent the last major contributors to the HS, as shown by the O···H/H···O plot, accounting for 9.5% of the whole surface. The remaining contact types are less significant and occupy 2% or less of the HS; a complete account of the intermolecular interactions is provided in Figure 4. Details on HS-**I** and specific data regarding the contact enrichments are provided in the Supplementary Materials.

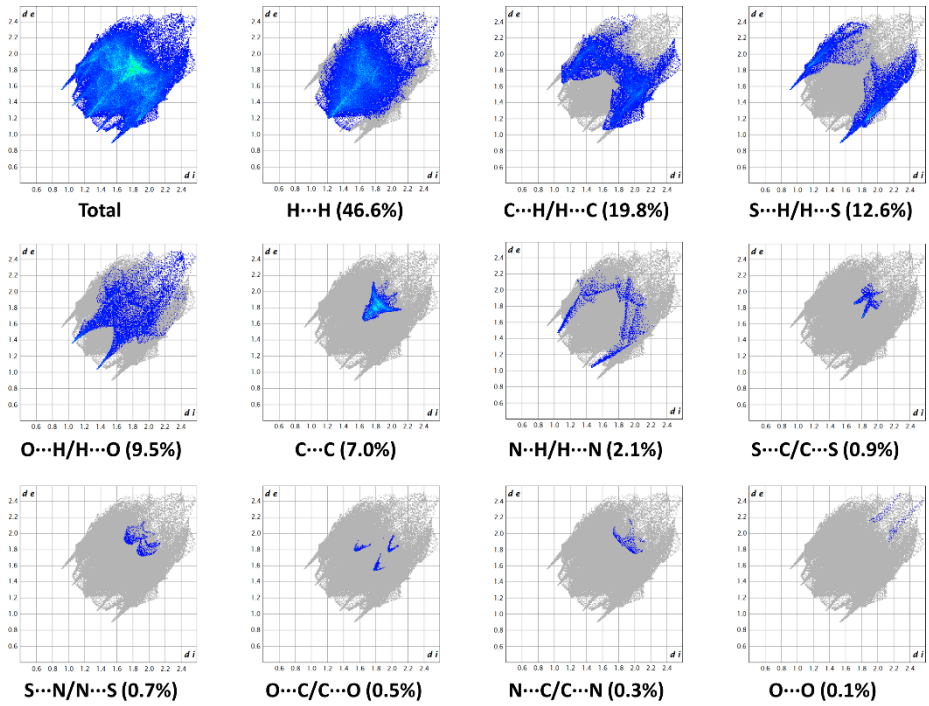

Figure 4. 2D Fingerprint plots of HS-**II**, providing a visual summary of the frequency of each combination of d_e and d_i across the HS. Points with a contribution to the surface are colored blue for a small contribution to green for a great contribution.

3.4 Biological assays

Initially, the antibacterial activity of the compound was screened by the agar disc diffusion assay. Results were compared with the antibacterial activity of known antibiotics (cefotaxime and ceftriaxone) [68]. As shown in Table 4, the bacterial cultures demonstrated a high susceptibility to the test compound, compared to the antibiotics. The highest antibacterial activity was observed against *S. aureus* (34 mm). Most notably, the compound performed better than the established antibiotics. Moreover, the antibacterial activity of the compound was equal to that of ceftriaxone in the case of *K. pneumoniae*, while it was lower than that of cefotaxime. The control containing DMSO did not affect the growth of the above mentioned gram-positive and gram-negative bacteria.

Table 4. Antibacterial activity of compound **4**.

P. aeruginosa			**4**			cefotaxime	ceftriaxone
Concentration (µg/mL)	125	250	500	1000	1500	1500	1500
Inhibition zone (mm)	3	9	20	31	40	34	30

S. aureus			**4**			cefotaxime	ceftriaxone
Concentration (µg/mL)	62.5	125	250	500	1000	1000	1000
Inhibition zone (mm)	2	6	12	22	34	26	17

E. coli			**4**			cefotaxime	ceftriaxone
Concentration (µg/mL)	125	250	500	1000	1500	1500	1500
Inhibition zone (mm)	3	7	16	26	33	25	20

A. baumanii			**4**			cefotaxime	ceftriaxone
Concentration (µg/mL)	125	250	500	1000	1500	1500	1500
Inhibition zone (mm)	2	5	15	23	29	24	16

K. pneumoniae			**4**			cefotaxime	ceftriaxone
Concentration (µg/mL)	500	1000	1500	2000	2500	2500	2500
Inhibition zone (mm)	2	5	11	16	23	32	24

The minimum inhibitory concentration (MIC) of the compounds against the test cultures (*S. aureus, E. coli, A. baumannii, P. aeruginosa,* and *K. pneumonia*) was determined using the microdilution method and the resazurin dye, after an initial screening [53]. The results were compared to those obtained with the control antibiotics (cefotaxime and ceftriaxone). Interestingly, the bacterial strains were more sensitive to **4** than to the controls (Table 5). *S. aureus* was the most susceptible, with a MIC value of 62.5 µg/mL, whereas *E. coli, A. baumanii*, and *P.* aeruginosa showed the same value of 125 µg/mL. Finally, *K. pneumoniae* was the least sensitive to **4**, with a MIC value of 500 µg/mL, the same value obtained with ceftriaxone, but higher than that exhibited by cefotaxime (250 µg/mL).

Table 5. Minimum inhibitory concentration (MIC, µg/mL) of **4** compared to that of the control antibiotics.

Investigated sample	Bacterial strains				
	E. coli	*P. aeruginosa*	*S. aureus*	*A. baumannii*	*K. pneumonia*
4	125	125	62.5	125	500
cefotaxime	250	250	250	250	250
ceftriaxone	500	500	500	500	500

The antibacterial activity of some dihydropyrimidine derivatives was also evaluated in previous work from our research group [53]. In comparison with compound **16** from the mentioned study, **4** showed improved antibacterial activity against all bacterial strains. For instance, **16** was not active against *K. pneumonia* [53], while all the bacterial strains tested were susceptible to **4**. The improvement of the antibacterial effect of **4** may be related to its chemical structure. In particular, the phenanthrene ring could be responsible for its enhanced biological activity, since the antimicrobial effect of this moiety has been previously observed against a variety of infectious agents, including drug-resistant strains [88-90]. However, despite the antimicrobial activity of the phenanthrenes having been known since the 1980s, the mechanism by which they act has not been properly studied yet [91].

Conversely, the potent antibacterial action of dihydropyrimidines can be explained by their ability to cross the bacterial cell wall. Moreover, they have been suggested to bind and inhibit a variety of enzymes (dihydrofolate reductase, bacterial DNA gyrase, aminoacyl-tRNA synthetases, etc.) [53, 92].

3.5 Computational studies

The key moieties of organic molecules can be identified and examined by theoretical

calculations [54]. For this purpose, the necessary quantum chemical parameters of the title compound **4** were determined by the Gaussian package program and are given in Table 6. The optimized structure of **4** is shown in Figure 5.

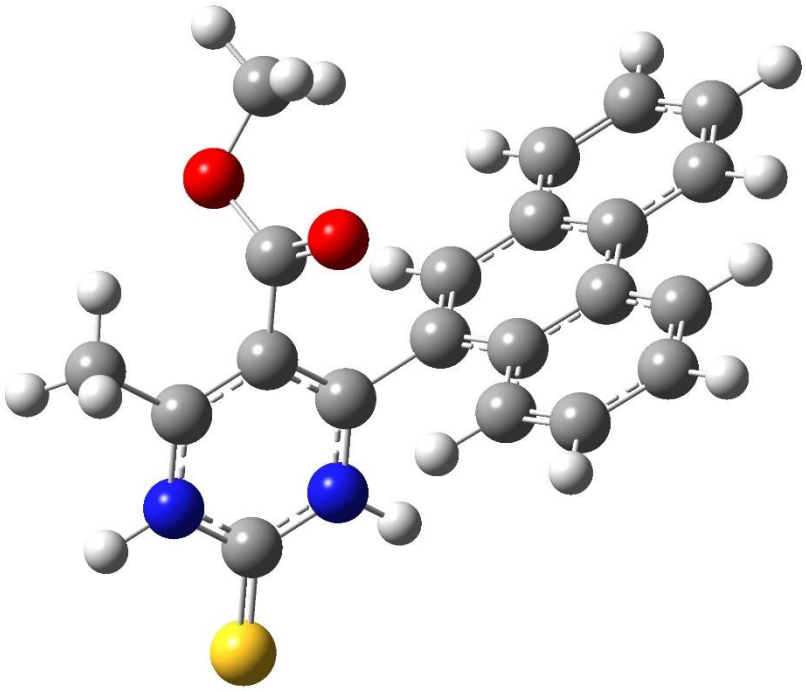

Figure 5. Optimized structure of **4**.

Among these parameters, the Lowest Unoccupied Molecular Orbital (LUMO) and Highest Occupied Molecular Orbital (HOMO) provide information about the reactivities of molecules. More precisely, the numerical value of these indicators describes charge-exchange properties. In detail, the HOMO parameter indicates the electron-donating ability of a compound; the more positive the value, the greater its tendency to donate electrons [55]. Conversely, the LUMO parameter describes the ability to withdraw electrons; the more negative the value, the greater the tendency to accept electrons [79].

Table 6. Calculated quantum chemical parameters of **4**.

Parameters	**Value**
E_{HOMO}	-4.0396
E_{LUMO}	-1.4033
I	4.0396
A	1.4033
ΔE	2.6363
η	1.3181
σ	0.7587
χ	2.7214
Pİ	-2.7214
ω	2.8094
ε	0.3560
Dipol	4.4536
Energy	-39956.1361

The HOMO-LUMO energy gap is another parameter that can be used to explain the reactivity: a small numerical value is usually correlated with a higher reactivity. The images of

HOMO, LUMO, and ΔE energy values of **4** are depicted in Figure 6. The electronegativity is yet another significant parameter; as with the previous one, a small numerical value indicates a higher reactivity. All data are reported in Table 6.

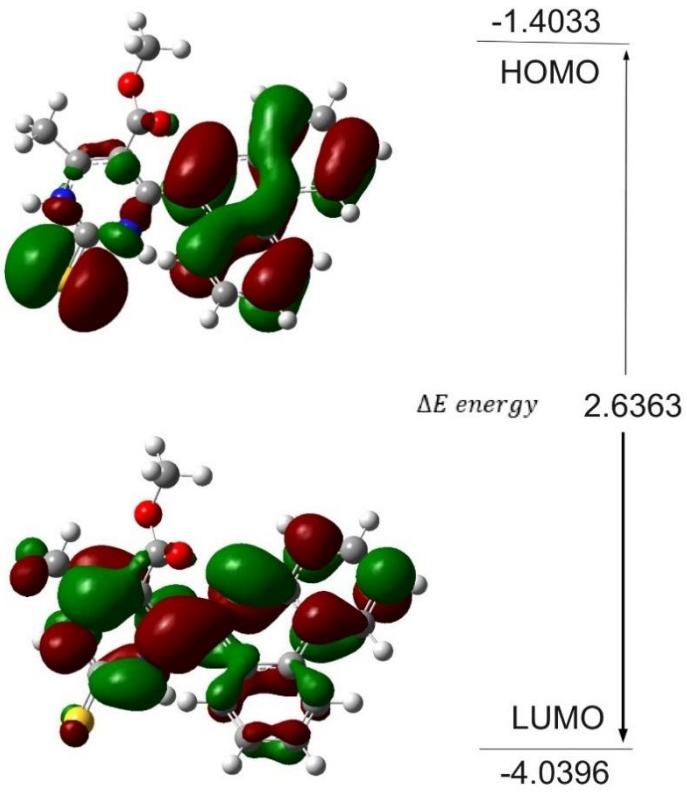

Figure 6. The images of HOMO, LUMO, and ΔE energy values of **4**.

Furthermore, the electrostatic potential (ESP) of **4** was calculated to determine the electron density of the molecule (Figure 7). Red regions are the richest in terms of electron density, blue-colored areas are electron-poor, and green parts indicate no-load zones. Electron-rich regions have a high propensity to donate electrons, while electron-poor areas show the highest electron-accepting ability. Therefore, red- and blue-colored regions indicate the most reactive sites of the molecule [70, 80].

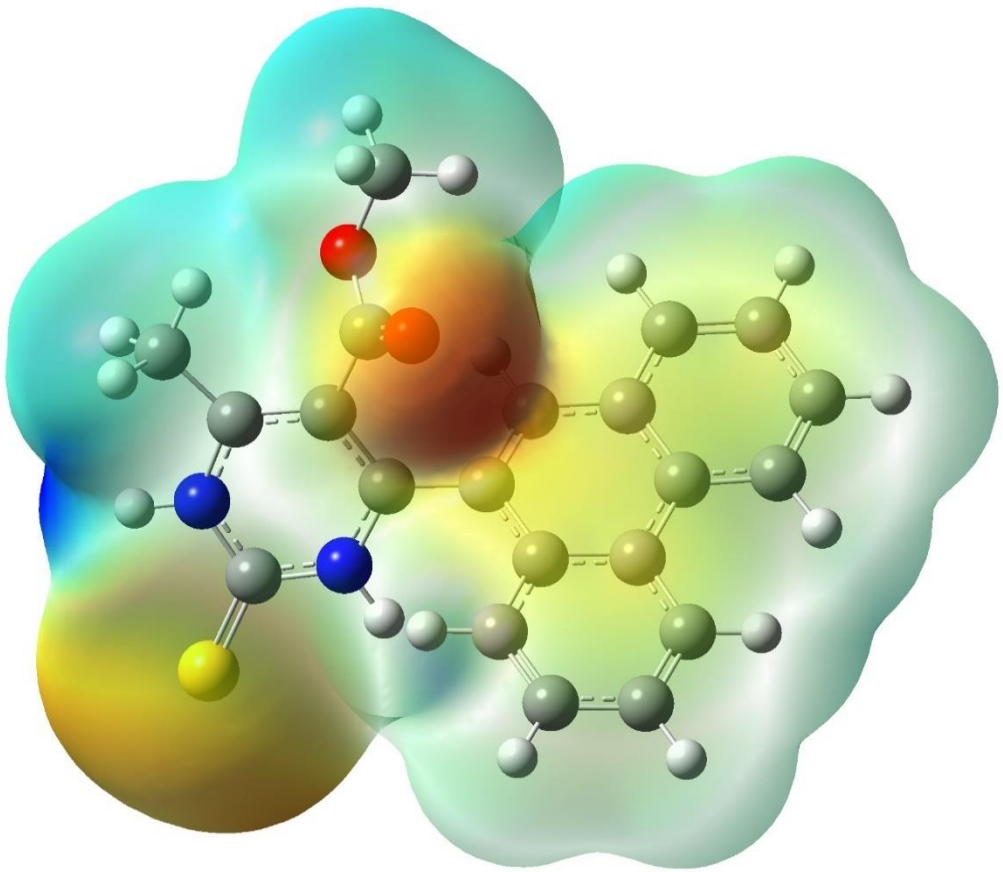

Figure 7. ESP of compound **4**.

The IR spectrum of **4** was calculated on the B3lyp/6-31g(d) basis set (Figure 8). The vibrations occurring at 3021 and 3202 cm^{-1} indicate aromatic C-H bonds. C-C bond vibrations are observed at an average of 1800 cm^{-1}, C-O signals are in the range of 1420-1430 cm^{-1}, and C=C bond vibrations are at 1220-1240 cm^{-1}.

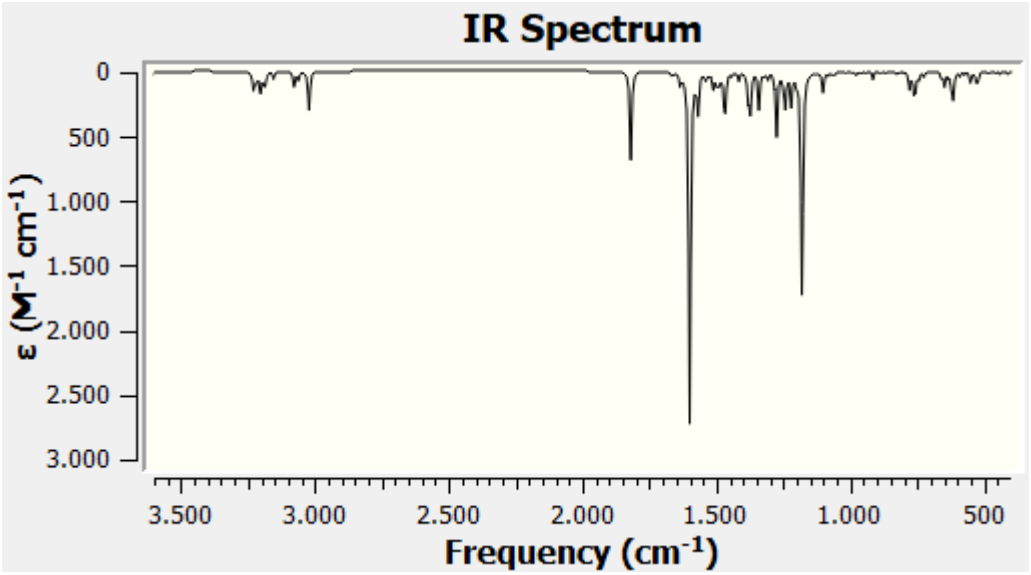

Figure 8. IR spectrum of **4**.

NMR chemical shifts of the carbon and hydrogen atoms of **4** were calculated by using the gauge-independent atomic orbital (GIAO) method [81]. The NMR spectrum of the compound

was calculated on the B3lyp/6-31g(d) basis set. The calculated chemical shift values are given in Table S1. ^{13}C signals below 51 ppm indicate aliphatic carbon atoms, while the others correspond to aromatic carbons. As for the ^{1}H spectrum, signals with chemical shift values between 5-8.5 ppm indicate aromatic hydrogens, while chemical shifts in the range of 1.4-3.7 ppm are observed for hydrogens attached to aliphatic carbons. The obtained data were in agreement with the experimental results.

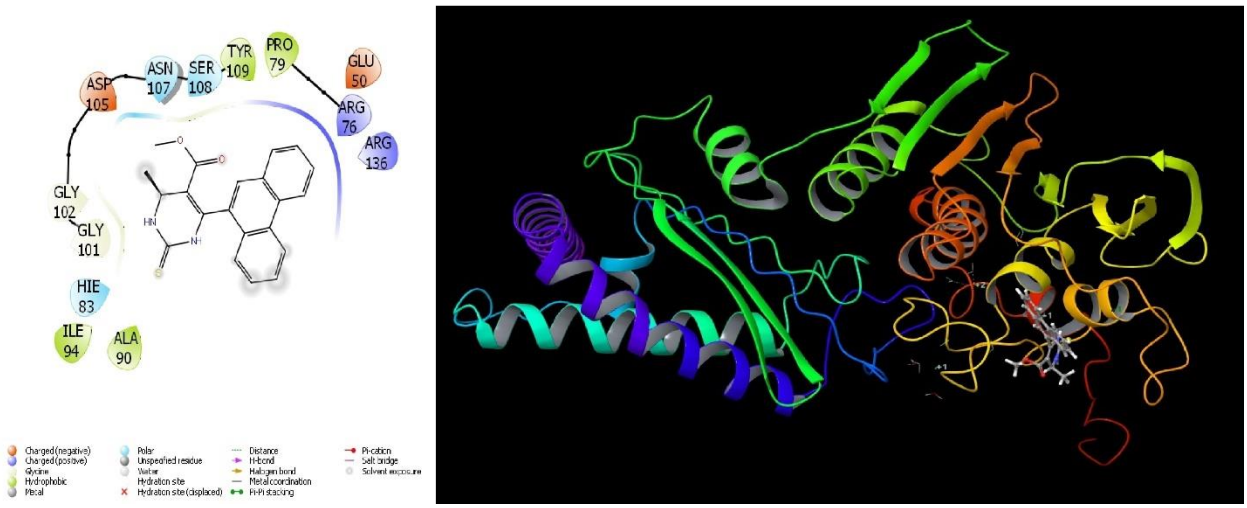

Figure 9. Interactions of **4** with the **4WUB** protein.

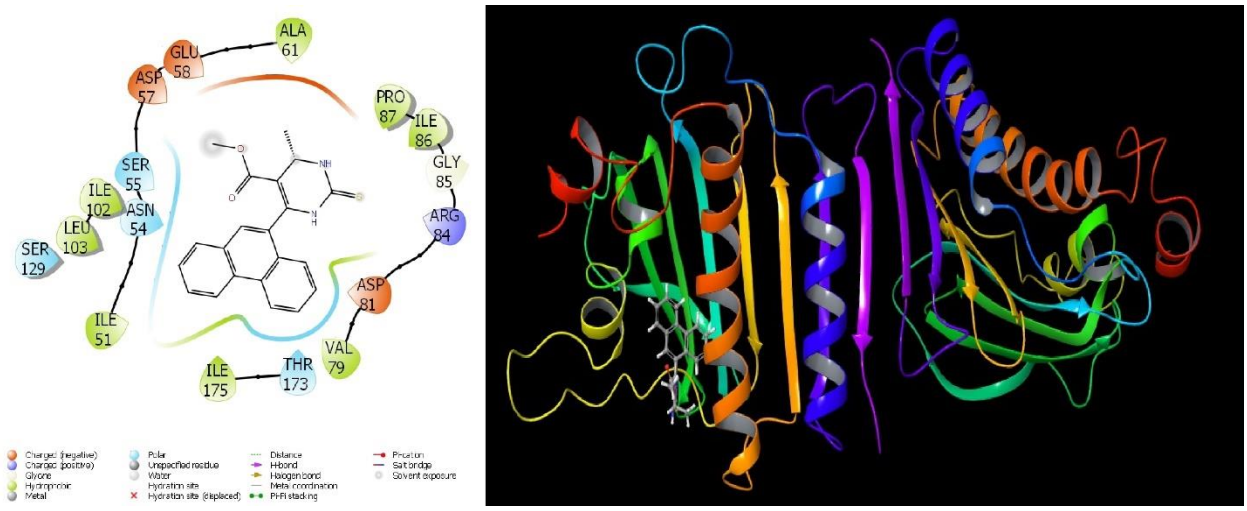

Figure 10. Interactions of **4** with the **3G7B** protein.

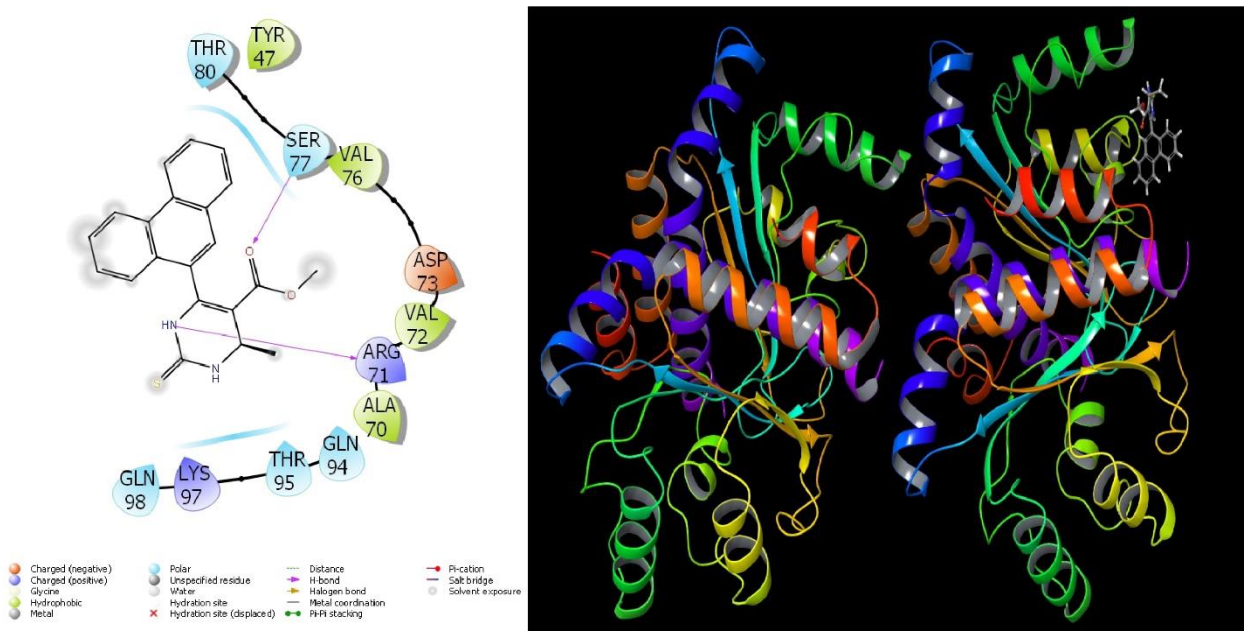

Figure 11. Interactions of **4** with the **2UV0** protein.

Molecular docking calculations were performed to investigate the possible binding of **4** to selected proteins from *Staphylococcus aureus*, *Pseudomonas aeruginosa*, and *Escherichia coli* (Figures 9-11).

Table 7. Numerical values of the docking parameters calculated for **4** and for the control antibiotics against the selected bacterial enzymes.

4WUB	**4**	**Ceftriaxone**	**Cefotaxime**
Docking Score	-4.98	-4.76	-4.38
Glide ligand efficiency	-0.19	-0.13	-0.15
Glide hbond	0.00	-0.35	-0.53
Glide evdw	-33.79	-36.44	-35.83
Glide ecoul	-3.10	-9.34	-4.18
Glide emodel	-46.27	-56.97	-48.69
Glide energy	-36.89	-45.78	-40.01
Glide einternal	3.07	8.03	6.28
Glide posenum	89	114	315
3G7B	**4**	**Ceftriaxone**	**Cefotaxime**
Docking Score	-5.88	-5.42	-4.79
Glide ligand efficiency	-0.23	-0.18	-0.13
Glide hbond	0.00	-0.46	-0.45
Glide evdw	-37.12	-39.35	-33.35
Glide ecoul	-1.11	-9.99	-8.33
Glide emodel	-50.82	-59.20	-50.93
Glide energy	-38.23	-49.33	-41.67
Glide einternal	1.99	15.79	7.18
Glide posenum	399	9	240
2UV0	**4**	**Ceftriaxone**	**Cefotaxime**
Docking Score	-4.95	-4.63	-3.46
Glide ligand efficiency	-0.19	-0.13	-0.12
Glide hbond	-0.35	-0.94	-0.48
Glide evdw	-25.53	-21.72	-22.51
Glide ecoul	-7.24	-15.18	-9.03
Glide emodel	-41.20	-47.41	-38.34
Glide energy	-32.78	-36.90	-31.54
Glide einternal	0.41	9.57	3.31
Glide posenum	300	232	280

All calculated docking parameters are given in Table 7. Among these indicators, Glide ligand efficiency, Glide hbond, Glide evdw, and Glide ecoul illustrate the efficiency of the molecule and provide a numerical value to define the chemical interactions (hydrogen bonds, polar and hydrophobic interactions, π-π and halogen contacts) [82]. On the other hand, parameters such as Glide emodel, Glide energy, Glide einternal, and Glide posenum describe the pose of the molecule within the active site of the protein [75]. Interestingly, the examination of the interaction of **4** with the selected proteins suggests it may perform better as a binder compared to the reference substances, ceftriaxone and cefotaxime.

The analysis of the druglikeness is fundamental to verify that a molecule is suitable to be further developed as a therapeutic agent [83]. Hence, an ADME/T (Absorption, Distribution, Metabolism, Excretion and Toxicity) study was performed to simulate the absorption of the molecule, its interaction with the human metabolic enzymes, and its excretion. All parameters obtained from these calculations are given in Table 8.

Table 8. ADME properties of **4**.

	4	**Reference Range**
mol_MW	362	130-725
dipole (D)	3.7	1.0-12.5
SASA	585	300-1000
FOSA	146	0-750
FISA	59	7-330
PISA	301	0-450
WPSA	79	0-175
volume (A^3)	1078	500-2000
donorHB	0	0-6
accptHB	2.5	2.0-20.0
glob (Sphere =1)	0.9	0.75-0.95
QPpolrz (A^3)	38.6	13.0-70.0
QPlogPC16	11.4	4.0-18.0
QPlogPoct	14.6	8.0-35.0
QPlogPw	5.6	4.0-45.0
QPlogPo/w	5.4	-2.0-6.5
QPlogS	-6.0	-6.5-0.5
CIQPlogS	-6.7	-6.5-0.5
QPlogHERG	-5.1	*
QPPCaco (nm/sec)	2708	**
QPlogBB	0.1	-3.0-1.2
QPPMDCK (nm/sec)	3920	**
QPlogKp	-1.4	Kp in cm/hr
IP (ev)	8.6	7.9-10.5
EA (eV)	1.0	-0.9-1.7
#metab	1	1-8
QPlogKhsa	1.0	-1.5-1.5
Human Oral Absorption	3	-
Percent Human Oral Absorption	100	***
PSA	64	7-200
Rule-Of-Five	1	Maximum is 4
Rule-Of-Three	1	Maximum is 3
Jm	0.0	-

*below -5, **<25 is poor and >500 is great, *** <25% is poor and >80% is high.

Some of them are related to the chemical characteristics of the molecule and some are linked to its biological properties. In detail, two indicators are instrumental to determine whether a compound has the potential to be drug, namely the Rule-Of-Five [84, 85], also known as the Lipinski's (or Pfizer's) Rule-Of-Five, and the Rule-Of-Three [86], also known as the Jorgensen's Rule-of-Three. The numerical value of these parameters should be as close to zero as possible (no violations); in the present case, **4** shows only 1 violation. However, its passage through the blood-brain and blood-intestinal barriers is predicted to occur with difficulty.

4. Conclusion

A new dihydropyrimidine derivative (**4**) was synthesized by the Biginelli reaction under microwave irradiation in the presence of cerium chloride. Its structure was investigated by SC-XRD and examined by Hirshfeld surface analysis to gain insights into the crystal packing and molecular interactions. Considering its potential antibacterial effect, **4** was tested against Gram-positive (*S. aureus*) and Gram-negative (*A. baumannii, E. coli, P.aeruginosa, K. pneumoniae*) bacteria. Interestingly, it was found to be more active than known antibiotics (ceftriaxone and cefotaxime) against *S. aureus, A. baumannii, E. coli, and P. aeruginosa.* Finally, the chemical properties and biological effects of the molecule were estimated through theoretical calculations. Molecular docking simulations revealed that the activity of **4** may be potentially higher than that of the reference antibiotics. In addition, the IR and NMR spectra of the compound were examined theoretically and were found to agree with the experimental results. The estimation of the druglikeness of **4** also provided promising results. As a result of our investigations, we believe that the data presented here will prove pivotal for the future *in vitro* and *in vivo* development of this class of compounds. The obtained results are encouraging, indicating that the synthesized dihydropyrimidine derivative indeed represents an interesting potential drug candidate with antibacterial activity.

Conflict of Interest

The authors declare no conflict of interest.

Funding

This work was supported by the Erasmus + overseas/ICM KA107 program and by the Scientific Research Project Fund of Sivas Cumhuriyet University under the project number RGD-020. This research was made possible by TUBITAK ULAKBIM, High Performance and Grid Computing Center (TR-Grid e-Infrastructure).

References

1. Bienaymé, H., Hulme, C., Oddon, G., & Schmitt, P. (2000). Maximizing synthetic efficiency: Multi- component transformations lead the way. *Chemistry–A European Journal*, *6*(18), 3321-3329. **https://doi.org/10.1002/1521-3765(20000915)6:18<3321::AID-CHEM3321>3.0.CO;2-A**
2. Zhu, J., & Bienaymé, H. (Eds.). (2006). *Multicomponent reactions*. John Wiley & Sons.

3. C.O. Kappe. "Recent advances in the Biginelli dihydropyrimidine synthesis. New tricks from an old dog", Accounts of Chemical Research 33.12 (2000): 879-888. https://doi.org/10.1021/ar000048h
4. N. Honnappa, A. Mukhopadhyay and J.N. Moorthy. "Biginelli reaction: an overview", Tetrahedron Letters 57.47 (2016): 5135-5149. https://doi.org/10.1016/j.tetlet.2016.09.047
5. W. Jie-Ping, Y. Liu. "Synthesis of dihydropyrimidinones and thiones by multicomponent reactions: strategies beyond the classical Biginelli reaction", Synthesis 2010.23 (2010): 3943-3953. DOI: 10.1055/s-0030-1258290
6. E. Woerly. "The Biginelli Reaction: Development and Application", Organic chemistry seminar at the University of Illinois, 2008: 1-8. http://www.chemistry.illinois.edu/research/organic/seminar_abstracts/seminar_abstracts_2008_2009.html.
7. C.O. Kappe. "100 Years of the Biginelli Dihydropyrimidine Synthesis", Tetrahedron 1993, 49, 6937-6963. https://doi.org/10.1016/S0040-4020(01)87971-0
8. S.S. Jagir "Past, present and future of the Biginelli reaction: a critical perspective." ARKIVOC: Online Journal of Organic Chemistry (2012): 66-133. http://dx.doi.org/10.3998/ark.5550190.0013.103
9. A.M. Maharramov, et al. "Synthesis, investigation of the new derivatives of dihydropyrimidines and determination of their biological activity", Journal of Molecular Structure 1141 (2017): 39-43. https://doi.org/10.1016/j.molstruc.2017.03.084
10. Trivedi, Amit R., et al. "Novel dihydropyrimidines as a potential new class of antitubercular agents." Bioorganic & medicinal chemistry letters 20.20 (2010): 6100-6102. https://doi.org/10.1016/j.bmcl.2010.08.046
11. Terracciano, Stefania, et al. "Structural insights for the optimization of dihydropyrimidin-2 (1 H)-one based mPGES-1 inhibitors." ACS medicinal chemistry letters 6.2 (2015): 187-191. https://doi.org/10.1021/ml500433j
12. (a) Folkers, Karl, and Treat B. Johnson. "Researches on Pyrimidines. CXXXVI. The Mechanism of Formation of Tetrahydropyrimidines by the Biginelli Reaction1." Journal of the American Chemical Society 55.9 (1933): 3784-3791. https://doi.org/10.1021/ja01336a054; (b) Sweet, Frederick, and John D. Fissekis. "Synthesis of 3, 4-dihydro-2 (1H)-pyrimidinones and the mechanism of the Biginelli reaction." Journal of the American Chemical Society 95.26 (1973): 8741-8749. https://doi.org/10.1021/ja00807a040; (c) Kappe, C. Oliver. "A reexamination of the mechanism of the Biginelli dihydropyrimidine synthesis. Support for an N-Acyliminium ion intermediate1." The Journal of organic chemistry 62.21 (1997): 7201-7204. https://doi.org/10.1021/jo971010u; (d) De Souza, Rodrigo OMA, et al. "The three- component Biginelli reaction: a combined experimental and theoretical mechanistic investigation." Chemistry–A European Journal 15.38 (2009): 9799-9804. **https://doi.org/10.1002/chem.200900470**; (e) Ramos, Luciana M., et al. "Mechanistic studies on Lewis acid catalyzed Biginelli reactions in ionic liquids: Evidence for the reactive intermediates and the role of the reagents." The Journal of organic chemistry 77.22 (2012): 10184-10193. https://doi.org/10.1021/jo301806n; (f) Puripat, Maneeporn, et al. "The Biginelli reaction is a urea-catalyzed organocatalytic multicomponent reaction." The Journal of organic chemistry 80.14 (2015): 6959-6967.https://doi.org/10.1021/jo301806n

13. Lewis, Ryan W., et al. "Dihydropyrimidinone positive modulation of δ-subunit-containing γ-aminobutyric acid type A receptors, including an epilepsy-linked mutant variant." Biochemistry 49.23 (2010): 4841-4851. https://doi.org/10.1021/bi100119t
14. Patil, Ashok D., et al. "Novel alkaloids from the sponge Batzella sp.: inhibitors of HIV gp120-human CD4 binding." The Journal of Organic Chemistry 60.5 (1995): 1182-1188.
15. Sehon, Clark A., et al. "Potent, selective and orally bioavailable dihydropyrimidine inhibitors of Rho kinase (ROCK1) as potential therapeutic agents for cardiovascular diseases." Journal of medicinal chemistry 51.21 (2008): 6631-6634. https://doi.org/10.1021/jm8005096
16. Alam, Ozair, et al. "Antihypertensive activity of newer 1, 4-dihydro-5-pyrimidine carboxamides: Synthesis and pharmacological evaluation." European journal of medicinal chemistry 45.11 (2010): 5113-5119. https://doi.org/10.1016/j.ejmech.2010.08.022
17. Chikhale, R. V., et al. "Synthesis and pharmacological investigation of 3-(substituted 1-phenylethanone)-4-(substituted phenyl)-1, 2, 3, 4-tetrahydropyrimidine-5-carboxylates." European journal of medicinal chemistry 44.9 (2009): 3645-3653. https://doi.org/10.1016/j.ejmech.2009.02.021
18. Zorkun, Inci Selin, et al. "Synthesis of 4-aryl-3, 4-dihydropyrimidin-2 (1H)-thione derivatives as potential calcium channel blockers." Bioorganic & medicinal chemistry 14.24 (2006): 8582-8589. https://doi.org/10.1016/j.bmc.2006.08.031
19. Atwal, Karnail S., et al. "Dihydropyrimidine calcium channel blockers: 2-heterosubstituted 4-aryl-1, 4-dihydro-6-methyl-5-pyrimidinecarboxylic acid esters as potent mimics of dihydropyridines." Journal of medicinal chemistry 33.5 (1990): 1510-1515. https://doi.org/10.1021/jm00167a035
20. Marathwada, Babasaheb Ambedkar. "Synthesis and anti-inflammatory activity of some [2-amino-6-(4-substituted aryl)-4-(4-substituted phenyl)-1, 6-dihydropyrimidine-5-yl]-acetic acid derivatives." Acta Pharm 53 (2003): 223-229.
21. Bahekar, Sushilkumar S., and Devanand B. Shinde. "Synthesis and anti-inflammatory activity of some [4, 6-(4-substituted aryl)-2-thioxo-1, 2, 3, 4-tetrahydro-pyrimidin-5-yl]-acetic acid derivatives." Bioorganic & medicinal chemistry letters 14.7 (2004): 1733-1736. https://doi.org/10.1016/j.bmcl.2004.01.039
22. Mokale, Santosh N., et al. "Synthesis and anti-inflammatory activity of some 3-(4, 6-disubtituted-2-thioxo-1, 2, 3, 4-tetrahydropyrimidin-5-yl) propanoic acid derivatives." Bioorganic & medicinal chemistry letters 20.15 (2010): 4424-4426. https://doi.org/10.1016/j.bmcl.2010.06.058
23. (a) Homan, Kristoff T., et al. "Identification and structure–function analysis of subfamily selective g protein-coupled receptor kinase inhibitors." ACS chemical biology 10.1 (2015): 310-319.https://doi.org/10.1021/cb5006323; (b) Waldschmidt, Helen V., et al. "Structure-based design, synthesis, and biological evaluation of highly selective and potent G protein-coupled receptor kinase 2 inhibitors." Journal of medicinal chemistry 59.8 (2016): 3793-3807. https://doi.org/10.1021/acs.jmedchem.5b02000
24. (a) Akhaja, Tarunkumar Nanjibhai, and Jignesh Priyakant Raval. "1, 3-Dihydro-2H-indol-2-ones derivatives: Design, synthesis, in vitro antibacterial, antifungal and antitubercular study." European

journal of medicinal chemistry 46.11 (2011): 5573-5579. https://doi.org/10.1016/j.ejmech.2011.09.023; (b) Yadlapalli, Rama Krishna, et al. "Synthesis and in vitro anticancer and antitubercular activity of diarylpyrazole ligated dihydropyrimidines possessing lipophilic carbamoyl group." Bioorganic & medicinal chemistry letters 22.8 (2012): 2708-2711. https://doi.org/10.1016/j.bmcl.2012.02.101

25. (a) October, Natasha, et al. "Reversed Chloroquines Based on the 3, 4- Dihydropyrimidin- 2 (1H)-one Scaffold: Synthesis and Evaluation for Antimalarial, β- Haematin Inhibition, and Cytotoxic Activity." ChemMedChem: Chemistry Enabling Drug Discovery 3.11 (2008): 1649-1653. **https://doi.org/10.1002/cmdc.200800172**; (b) Fatima, Seerat, et al. "One pot efficient diversity oriented synthesis of polyfunctional styryl thiazolopyrimidines and their bio-evaluation as antimalarial and anti-HIV agents." European journal of medicinal chemistry 55 (2012): 195-204. https://doi.org/10.1016/j.ejmech.2012.07.018; (c) Kaur, Hardeep, et al. "Primaquine–pyrimidine hybrids: synthesis and dual-stage antiplasmodial activity." European journal of medicinal chemistry 101 (2015): 266-273. https://doi.org/10.1016/j.ejmech.2015.06.045
26. (a) Wang, Anqi, et al. "New magnetic nanocomposites of ZrO_2–Al_2O_3–Fe_3O_4 as green solid acid catalysts in organic reactions." Catalysis Science & Technology 4.1 (2014): 71-80. DOI: 10.1039/C3CY00572K ; (b) Ghosh, Barun Kumar, Subhenjit Hazra, and Narendra Nath Ghosh. "Synthesis of Cu@ CF@ SBA15: A Versatile catalysts for (i) reduction of dyes, trifluralin, Synthesis of (ii) DHPMs by Biginelli reaction and (iii) 1, 2, 3-triazole derivatives by 'Click reaction'." Catalysis Communications 80 (2016): 44-48. https://doi.org/10.1016/j.catcom.2016.03.016
27. Ibrahim, Diaa A., and Amira M. El-Metwally. "Design, synthesis, and biological evaluation of novel pyrimidine derivatives as CDK2 inhibitors." European journal of medicinal chemistry 45.3 (2010): 1158-1166. https://doi.org/10.1016/j.ejmech.2009.12.026
28. Kumar, BR Prashantha, et al. "Novel Biginelli dihydropyrimidines with potential anticancer activity: a parallel synthesis and CoMSIA study." European journal of medicinal chemistry 44.10 (2009): 4192-4198. https://doi.org/10.1016/j.ejmech.2009.05.014
29. Agbaje, Oluropo C., et al. "Synthesis and in vitro cytotoxicity evaluation of some fluorinated hexahydropyrimidine derivatives." Bioorganic & medicinal chemistry letters 21.3 (2011): 989-992.https://doi.org/10.1016/j.bmcl.2010.12.022
30. Wright, Christine M., et al. "Pyrimidinone-peptoid hybrid molecules with distinct effects on molecular chaperone function and cell proliferation." Bioorganic & medicinal chemistry 16.6 (2008): 3291-3301. https://doi.org/10.1016/j.bmc.2007.12.014
31. Kaan, Hung Yi Kristal, et al. "Structural basis for inhibition of Eg5 by dihydropyrimidines: stereoselectivity of antimitotic inhibitors enastron, dimethylenastron and fluorastrol." Journal of medicinal chemistry 53.15 (2010): 5676-5683. https://doi.org/10.1021/jm100421n
32. Klein, Emmanuel, et al. "New chemical tools for investigating human mitotic kinesin Eg5." Bioorganic & medicinal chemistry 15.19 (2007): 6474-6488. https://doi.org/10.1016/j.bmc.2007.06.016

33. (a) Zhu, Xuejun, et al. "2, 4-Diaryl-4, 6, 7, 8-tetrahydroquinazolin-5 (1H)-one derivatives as anti-HBV agents targeting at capsid assembly." Bioorganic & medicinal chemistry letters 20.1 (2010): 299-301. https://doi.org/10.1016/j.bmcl.2009.10.119; (b) Dhumaskar, Kashinath L., et al. "Graphite catalyzed solvent free synthesis of dihydropyrimidin-2 (1H)-ones/thiones and their antidiabetic activity." Bioorganic & medicinal chemistry letters 24.13 (2014): 2897-2899. https://doi.org/10.1016/j.bmcl.2014.04.099; (c) Treptow, Tamara GM, et al. "Novel hybrid DHPM-fatty acids: synthesis and activity against glioma cell growth in vitro." European journal of medicinal chemistry 95 (2015): 552-562. https://doi.org/10.1016/j.ejmech.2015.03.062; (d) Chikhale, Rupesh, et al. "Development of selective DprE1 inhibitors: Design, synthesis, crystal structure and antitubercular activity of benzothiazolylpyrimidine-5-carboxamides." European journal of medicinal chemistry 96 (2015): 30-46. https://doi.org/10.1016/j.ejmech.2015.04.011; (e) Rashid, Umer, et al. "Structure based medicinal chemistry-driven strategy to design substituted dihydropyrimidines as potential antileishmanial agents." European journal of medicinal chemistry 115 (2016): 230-244. https://doi.org/10.1016/j.ejmech.2016.03.022; (f) Singh, Kamaljit, and Tavleen Kaur. "Pyrimidine-based antimalarials: design strategies and antiplasmodial effects." MedChemComm 7.5 (2016): 749-768. **https://doi.org/10.1039/C6MD00084C**

34. Barrow, James C., et al. "In vitro and in vivo evaluation of dihydropyrimidinone C-5 amides as potent and selective α1A receptor antagonists for the treatment of benign prostatic hyperplasia." Journal of medicinal chemistry 43.14 (2000): 2703-2718. https://doi.org/10.1021/jm990612y

35. Singh, Brajesh K., et al. "Synthesis of 2-sulfanyl-6-methyl-1, 4-dihydropyrimidines as a new class of antifilarial agents." European journal of medicinal chemistry 43.12 (2008): 2717-2723. https://doi.org/10.1016/j.ejmech.2008.01.038

36. Zhu, Xuejun, et al. "2, 4-Diaryl-4, 6, 7, 8-tetrahydroquinazolin-5 (1H)-one derivatives as anti-HBV agents targeting at capsid assembly." Bioorganic & medicinal chemistry letters 20.1 (2010): 299-301. https://doi.org/10.1016/j.bmcl.2009.10.119

37. Lloyd, John, et al. "Dihydropyrazolopyrimidines containing benzimidazoles as KV1. 5 potassium channel antagonists." Bioorganic & medicinal chemistry letters 19.18 (2009): 5469-5473. https://doi.org/10.1016/j.bmcl.2009.07.083

38. Finlay, H. J., Lloyd, J., Vaccaro, W., Kover, A., Yan, L., Bhave, G., ... & DiMarco, J. (2012). Discovery of ((S)-5-(Methoxymethyl)-7-(1-methyl-1 H-indol-2-yl)-2-(trifluoromethyl)-4, 7-dihydropyrazolo [1, 5-a] pyrimidin-6-yl)((S)-2-(3-methylisoxazol-5-yl) pyrrolidin-1-yl) methanone As a Potent and Selective IKur Inhibitor. *Journal of medicinal chemistry*, *55*(7), 3036-3048. https://doi.org/10.1021/jm201386u

39. Lloyd, John, et al. "Pyrrolidine amides of pyrazolodihydropyrimidines as potent and selective KV1. 5 blockers." Bioorganic & medicinal chemistry letters 20.4 (2010): 1436-1439. https://doi.org/10.1016/j.bmcl.2009.12.085

40. G.C. Rovnyak, K.S. Atwal, A. Hedberg, S.D. Kimball, S. Moreland, J.Z. Gougoutas, B.C. O'Reilly, J. Schwartz, M.F. Malley. "Dihydropyrimidine calcium channel blockers. 4. Basic 3-substituted-4-aryl-1,4-dihydropyrimidine-5-carboxylic acid esters. Potent

antihypertensive agents", J. Med. Chem. 35 (17) (1992) 3254-3263, http://dx.doi.org/10.1021/jm00095a023.

41. Mayer, Thomas U., et al. "Small molecule inhibitor of mitotic spindle bipolarity identified in a phenotype-based screen." *Science* 286.5441 (1999): 971-974. DOI: 10.1126/science.286.5441.971
42. Yen Moore, Angela. "Clinical applications for topical 5-fluorouracil in the treatment of dermatological disorders." Journal of Dermatological Treatment 20.6 (2009): 328-335. https://doi.org/10.3109/09546630902789326
43. Janos, Fischer, and Ganellin C. Robin. "Analogue-based Drug Discovery." (2006): 490.
44. Garcia-Saez, Isabel, et al. "Structure of human Eg5 in complex with a new monastrol-based inhibitor bound in the R configuration." *Journal of Biological Chemistry* 282.13 (2007): 9740-9747. https://doi.org/10.1074/jbc.M608883200
45. Kaan, Hung Yi Kristal, et al. "Structural basis for inhibition of Eg5 by dihydropyrimidines: stereoselectivity of antimitotic inhibitors enastron, dimethylenastron and fluorastrol." *Journal of medicinal chemistry* 53.15 (2010): 5676-5683. https://doi.org/10.1021/jm100421n
46. Northrop-Clewes, Christine A., and David I. Thurnham. "The discovery and characterization of riboflavin." *Annals of Nutrition and Metabolism* 61.3 (2012): 224-230. https://doi.org/10.1159/000343111
47. WH, PRUSOFF. "Synthesis and biological activities of iododeoxyuridine, an analog of thymidine." *Biochimica et biophysica acta* 32.1 (1959): 295-296. DOI: 10.1016/0006-3002(59)90597-9
48. Wilhelmus, Kirk R. "Antiviral treatment and other therapeutic interventions for herpes simplex virus epithelial keratitis." *Cochrane Database of Systematic Reviews* 1 (2015). **https://doi.org/10.1002/14651858.CD002898.pub5**
49. Mader, Timothy J., et al. "A randomized controlled trial of intravenous aminophylline for atropine-resistant out- of- hospital asystolic cardiac arrest." *Academic emergency medicine* 10.3 (2003): 192-197. **https://doi.org/10.1197/aemj.10.3.192**
50. Crooks, James, et al. "Effect of pretreatment with methylthiouracil on results of 131I therapy." *British Medical Journal* 1.5167 (1960): 151. doi: 10.1136/bmj.1.5167.151
51. Huseynzada, A. E., et al. "Synthesis, crystal structure and antibacterial studies of 2, 4, 6-trimetoxybenzaldehyde based dihydropyrimidine derivatives." Journal of Molecular Structure 1241 (2021): 130678. https://doi.org/10.1016/j.molstruc.2021.130678
52. Huseynzada, A. E., et al. "Synthesis, crystal structure and antibacterial properties of 6-methyl-2-oxo-4-(quinolin-2-yl)-1, 2, 3, 4-tetrahydropyrimidine-5-carboxylate." *Journal of Molecular Structure* 1219 (2020): 128581. https://doi.org/10.1016/j.molstruc.2020.128581
53. Huseynzada, Alakbar E., et al. "Synthesis, crystal structure and antibacterial studies of dihydropyrimidines and their regioselectively oxidized products." *RSC Advances* 11.11 (2021): 6312-6329. **https://doi.org/10.1039/D0RA10255E**
54. Tüzün, B., & Saripinar, E. (2020). Molecular docking and 4D-QSAR model of methanone derivatives by electron conformational-genetic algorithm method. Journal of the Iranian Chemical Society, 17(5), 985-1000. https://doi.org/10.1007/s13738-019-01835-8

55. Gedikli, M. U. S. T. A. F. A., Tuzun, B. U. R. A. K., Aktas, A., Sayin, K. O. R. A. Y., & Ataseven, H. İ. L. M. İ. (2021). Are clarithromycin, azithromycin and their analogues effective in the treatment of COVID19. BRATISLAVA MEDICAL JOURNAL-BRATISLAVSKE LEKARSKE LISTY, 122(2). Doi: 10.4149/bll_2021_015
56. Ronkin, Steven M., et al. "Discovery of pyrazolthiazoles as novel and potent inhibitors of bacterial gyrase." Bioorganic & Medicinal Chemistry Letters 20.9 (2010): 2828-2831. https://doi.org/10.1016/j.bmcl.2010.03.052
57. Bottomley, M. J., Muraglia, E., Bazzo, R., & Carfi, A. (2007). Molecular insights into quorum sensing in the human pathogen Pseudomonas aeruginosa from the structure of the virulence regulator LasR bound to its autoinducer. Journal of Biological Chemistry, 282(18), 13592-13600. https://doi.org/10.1074/jbc.M700556200
58. Hearnshaw, S. J., Chung, T. H., Stevenson, C. E. M., Maxwell, A., & Lawson, D. M. (2015). The role of monovalent cations in the ATPase reaction of DNA gyrase. Acta Crystallographica Section D: Biological Crystallography, 71(4), 996-1005. https://doi.org/10.1107/S1399004715002916
59. GM. Sheldrick. SHELXTL V5.1, Software reference manual. Madison, Wisconsin: Bruker AXS Inc.; 1997, 1-250.
60. Farrugia, Louis J. "WinGX and ORTEP for Windows: an update." Journal of Applied Crystallography 45.4 (2012): 849-854. https://doi.org/10.1107/S0021889812029111
61. SJ, Macrae CF Sovago I. Cottrell. "Galek PTA McCabe P." Pidcock E. Platings M. Shields GP Stevens JS Towler M. Wood PA J. Appl. Crystallogr 53 (2020): 226-235.
62. Nardelli, M. "Parst: A system of fortran routines for calculating molecular structure parameters from results of crystal structure analyses." Computers & Chemistry 7.3 (1983): 95-98. https://doi.org/10.1016/0097-8485(83)85001-3
63. Turner, M. J., et al. "Crystal Explorer17. 2017." University of Western Australia. Available online: http://hirshfeldsurface. net (accessed on 18 February 2022) (2021).
64. Guillot, B. "Molecular recognition enrichment rules in crystals and protemin/ligand complexes." Acta Crystallogr., Sect. A: Found. Crystallogr 68 (2012): s204.
65. Martin, Anandi, et al. "A new rapid and simple colorimetric method to detect pyrazinamide resistance in Mycobacterium tuberculosis using nicotinamide." *Journal of Antimicrobial Chemotherapy* 58.2 (2006): 327-331. https://doi.org/10.1093/jac/dkl231
66. Israyilova, Aygun, et al. "Biochemical characterization of glutamate racemase—a new candidate drug target against Burkholderia cenocepacia infections." *PloS one* 11.11 (2016): e0167350. https://doi.org/10.1371/journal.pone.0167350
67. HAJIYEVA, SARVINAZ, et al. "The role of diazacrown ether in the enhancement of the biological activity of silver nanoparticles." *Turkish Journal of Chemistry* 43.6 (2019): 1711-1721. doi:10.3906/kim-1907-10
68. Mayrhofer, Sigrid, et al. "Comparison of broth microdilution, E -test, and agar disk diffusion methods for antimicrobial susceptibility testing of *Lactobacillus acidophilus* group members." *Applied and Environmental Microbiology* 74.12 (2008): 3745-3748. https://doi.org/10.1128/AEM.02849-07

69. Frisch, M. J., et al. "Gaussian 09, Revision D. 01, Gaussian, Inc., Wallingford CT." See also: URL: http://www. gaussian. com (2009).
70. Becke, A. "Density-functional thermochemistry. III. The role of exact exchange (1993) J." Chem. Phys 98: 5648.
71. Tüzün, B., & Sayin, K. (2019). Investigations over optical properties of boron complexes of benzothiazolines. Spectrochimica Acta Part A: Molecular and Biomolecular Spectroscopy, 208, 48-56. https://doi.org/10.1016/j.saa.2018.09.060
72. Schrödinger Release 2021-3: Maestro, Schrödinger, LLC, New York, NY, 2021.
73. Schrödinger Release 2019-4: Protein Preparation Wizard; Epik, Schrödinger, LLC, New York, NY, 2016; Impact, Schrödinger, LLC, New York, NY, 2016; Prime, Schrödinger, LLC, New York, NY, 2019.
74. Schrödinger Release 2021-3: LigPrep, Schrödinger, LLC, New York, NY, 2021.
75. Tuzun, B., Nasibova, T., Garaev, E., Sayin, K., & Ataseven, H. (2021). Could Peganum harmala be effective in the treatment of COVID-19?. Bratislavske Lekarske Listy, 122(9), 670-679. DOI: 10.4149/bll_2021_108
76. Schrödinger Release 2021-3: QikProp, Schrödinger, LLC, New York, NY, 2021.
77. Ciceri, Samuele, et al. "Vecuronium bromide and its advanced intermediates: A crystallographic and spectroscopic study." Steroids 176 (2021): 108928. https://doi.org/10.1016/j.steroids.2021.108928
78. Mori, Matteo, et al. "Synthesis and Characterization of a Tetradentate Bispidine-based Ligand and its Zinc (II) Complex." Inorganica Chimica Acta (2022): 120968. https://doi.org/10.1016/j.ica.2022.120968
79. Rezaeivala, M., Karimi, S., Tuzun, B., & Sayin, K. (2022). Anti-corrosion behavior of 2-((3-(2-morpholino ethylamino)-N3-((pyridine-2-yl) methyl) propylimino) methyl) pyridine and its reduced form on Carbon Steel in Hydrochloric Acid solution: Experimental and theoretical studies. Thin Solid Films, 741, 139036. https://doi.org/10.1016/j.tsf.2021.139036
80. Bilgiçli, Ahmet T., et al. "Tetra-substituted phthalocyanines bearing thiazolidine derivatives: synthesis, anticancer activity on different cancer cell lines, and molecular docking studies." Dalton Transactions 50.43 (2021): 15778-15792. DOI: 10.1039/D1DT02023D
81. Bilgicli, Ahmet T., et al. "Synthesis of (4R)- 2- (3- hydroxyphenyl) thiazolidine- 4- carboxylic acid substituted phthalocyanines: Anticancer activity on different cancer cell lines and molecular docking studies." Applied Organometallic Chemistry 35.7 (2021): e6242. https://doi.org/10.1002/aoc.6242
82. Cetiner, E., et al. "Could boron-containing compounds (BCCs) be effective against SARS-CoV-2 as anti-viral agent?." Bratislavske lekarske listy 122.4 (2021): 263-269. https://doi.org/10.4149/BLL_2021_44
83. Ataseven, H., et al. "Could boron compounds be effective against SARS-CoV-2?." Bratislavske Lekarske Listy 122.10 (2021): 753-758. https://doi.org/10.4149/BLL_2021_121
84. Lipinski, Christopher A. "Lead-and drug-like compounds: the rule-of-five revolution." Drug discovery today: Technologies 1.4 (2004): 337-341.

85. Lipinski, Christopher A., et al. "Experimental and computational approaches to estimate solubility and permeability in drug discovery and development settings." Advanced drug delivery reviews 23.1-3 (1997): 3-25.
86. Jorgensen, William L., and Erin M. Duffy. "Prediction of drug solubility from structure." Advanced drug delivery reviews 54.3 (2002): 355-366.
87. CLSI-Clinical Laboratory Standards Institute. Methods for dilution antimicrobial susceptibility test for bacteria that grow aerobically. Available online: http://www.clsi.org/source/orders/free/m07-a9.pdf (accessed on 18 September 2012).
88. Yoshikawa K., Baba C., Iseki K., Ito T., Asakawa Y., Kawano S., et al. Phenanthrene and phenylpropanoid constituents from the roots of Cymbidium Great Flower 'Marylaurencin' and their antimicrobial activity. *J. Nat. Med.* (2014), 68, 743–747. 10.1007/s11418-014-0854-8.
89. Tóth B., Hohmann J., Vasas A. Phenanthrenes: a promising group of plant secondary metabolites. *J. Nat. Prod.* (2018), 81, 661–678. 10.1021/acs.jnatprod.7b00619.
90. Qian C. D., Jiang F. S., Yu H. S., Fu Y. H., Cheng D. Q., Gan L. S., et al. Antibacterial Biphenanthrenes from the fibrous roots of *Bletilla striata*. *J. Nat. Prod.* (2015), 78, 939–943. 10.1021/np501012n.
91. Chen BC, Lin CX, Chen NP, Gao CX, Zhao YJ, Qian CD. Phenanthrene antibiotic targets bacterial membranes and kills *Staphylococcus aureus* with a low propensity for resistance development. *Front Microbiol* (2018), 9:1593. https://doi.org/10.3389/ fmicb.2018.01593.
92. Ahmad, M.J., Hassan, S.F., Nisa, R.U. *et al.* Synthesis, in vitro potential and computational studies on 2-amino-1, 4-dihydropyrimidines as multitarget antibacterial ligands. *Med Chem Res* **25,** 1877–1894 (2016). https://doi.org/10.1007/s00044-016-1613-z.